Available online at www.sciencedirect.com

ScienceDirect

www.elsevier.com/locate/jes

JES JOURNAL OF ENVIRONMENTAL SCIENCES www.jesc.ac.cn

Screening hydroxyapatite for cadmium and lead immobilization in aqueous solution and contaminated soil: The role of surface area

Hongying Li[1], *Xisheng Guo*[1], *Xinxin Ye*[1,2,*]

1. *Institute of Soil and Fertilizer, Anhui Academy of Agricultural Sciences, Hefei 230031, China*
2. *Key Laboratory of Materials Physics, Centre for Environmental and Energy Nanomaterials, Anhui Key Laboratory of Nanomaterials and Nanotechnology, Institute of Solid State Physics, Chinese Academy of Sciences, Hefei 230031, China*

ARTICLE INFO

Article history:
Received 25 January 2016
Revised 31 March 2016
Accepted 5 April 2016
Available online 2 May 2016

Keywords:
Hydroxyapatite
Cadmium
Lead
Remediation
Structure and morphology

ABSTRACT

Hydroxyapatite (HAP) has been widely used to immobilize many cationic metals in water and soils. The specific reason why an increase in the surface area of HAP enhances cadmium (Cd) uptake, but has no effect on lead (Pb) uptake, is not clear. The aim of this study was to determine the factors causing the differences in sorption behavior between Cd and Pb by evaluating HAPs with different surface areas. We synthesized HAPs with two different surface areas, which were characterized by X-ray diffraction, N_2 adsorption, and scanning electron microscopy, and then evaluated them as sorbents for Cd and Pb removal by testing in single and binary systems. The sorption capacity of large surface area HAP (1.85 mmol/g) for Cd in the single-metal system was higher than that of small surface area HAP (0.64 mmol/g), but there were no differences between single- and binary-metal solutions containing Pb. After the Cd experiments, the HAP retained a stable structure and intact morphology, which promotes the accessibility of reactive sites for Cd. However, a newly formed precipitate covered the surface and blocked the channels in the presence of Pb, which reduced the number of potential adsorption sites on HAP for Cd and Pb. Remediation experiments using Cd- and Pb-contaminated soil produced similar results to the solution tests. These results indicate that alterations of the structure and morphology during the reaction is an important factor influencing metal sorption to HAP.

Introduction

Hydroxyapatite (HAP) is low-cost, eco-friendly and highly effective stabilizing agent for a variety of metals, and is readily available in the natural environment (Leyva et al., 2001; Lusvardi et al., 2002; Seaman et al., 2001; Gray et al., 2006; Lee et al., 2009). Consequently, it has been widely used to immobilize various cationic metals in water and soil. In particular, the immobilization of toxic metal ions such as cadmium (Cd) and lead (Pb) has been extensively studied because of their large potential to harm human health and the environment (Ye et al., 2014, 2015). However, the physical properties of the HAP surface that influence Cd and Pb sorption remain insufficiently understood (Da Rocha et al., 2002; Baillez et al., 2007). In the case of Cd, some studies have shown that Cd adsorption by HAPs depends on the specific

* *Corresponding author*. E-mail: xxye@issp.ac.cn (Xinxin Ye).

http://dx.doi.org/10.1016/j.jes.2016.04.005
1001-0742/

surface area (Baillez et al., 2007; Zhang et al., 2010). These authors have reported that the maximum Cd^{2+} uptake by HAP was about 1.41 mmol/g with a specific surface area of 130 m^2/g (Zhang et al., 2010), 0.592 mmol/g with 77 m^2/g (Xu et al., 1994), 0.63 mmol/g with 74 m^2/g (Christoffersen et al., 1988), 0.432 mmol/g with 52 m^2/g (Mandjiny et al., 1995), and 0.21 mmol/g with 33 m^2/g (Da Rocha et al., 2002). However, no correlation was found between the maximum sorption capacity and specific surface area for Pb adsorption. According to Baillez et al. (2007), who studied three different HAP samples, the surface area had no influence on the maximum Pb^{2+} uptake (2.17 mmol/g with 41 m^2/g, 1.73 mmol/g with 104 m^2/g, and 1.59 mmol/g with 50 m^2/g). Zhang et al. (2010) reported on the effect of both Cd and Pb on the HAP sorption process in aqueous solution and found that competitive sorption between Pb and Cd on HAP existed in the binary system, and the inhibitive effect of Pb on Cd sorption by HAP was greater than that of Cd on Pb. Hence, studies still need to be conducted to determine the influence of the surface area on the hydroxyapatite sorption properties for Cd and Pb in single-metal and binary systems.

Different sorption mechanisms of HAP for Cd and Pb could produce the observed differences in adsorption results. Several stabilization mechanisms of Cd and Pb on HAP are known, including ion exchange, surface complexation, diffusion through the solid material, and dissolution–precipitation (Peld et al., 2004; Mandjiny et al., 1998; Sheha, 2007; Corami et al., 2008), with dissolution–precipitation being the dominant process in the immobilization of Pb (Sandrine et al., 2007; Jang et al., 2008). Ion-exchange and surface complexation are favored for the crystal structures and morphologies that consist of an adaptable framework, which are penetrated and diffused by channels along which ions migrate, with the stable and integral framework tending to facilitate the passage of ions through the tunnels (Srinivasan et al., 2006; Vila et al., 2011). If the processes of metal migration and diffusion are satisfied, maximizing the surface area is beneficial for physical sorption, ion exchange, and surface complexation as a result of enhancing the accessibility of contaminants to the surfaces. In contrast, the destruction of crystal structures and morphologies will prevent adsorption sites becoming available to contaminants during reactions. The dissolution–precipitation process may result in large modifications of the structure and surface morphology of HAP, resulting in a loss of porosity and a decrease in the number of effective reactive sites, which can strongly affect its sorption capacity. Therefore, the influence of Cd and Pb sorption on the surface physical properties of HAP needs to be further investigated to optimize metal capture in water and soil.

The aim of this study was to understand the influence of the surface area of HAP on the sorption efficiency in water and soil contaminated with Cd and Pb. A simple method was used to synthesize two HAP samples with different surface areas, namely large surface area HAP (LHAP) and small surface area HAP (SHAP). Laboratory batch sorption and soil immobilization experiments were conducted to quantify the effect of the HAP surface area on the sorption of Cd and Pb in single- and binary-metal systems. The specific objectives of this work were to: (1) describe the physical and chemical properties of LHAP and SHAP; (2) compare the sorption characteristics of Cd and Pb on LHAP and SHAP in terms of thermodynamic parameters; (3) determine the mechanisms underlying the sorption differences using different structural analysis techniques; and (4) determine the bioavailability of Cd and Pb in soil using a sequential extraction method.

1. Materials and methods

1.1. Materials

Two kinds of HAP, with different surface areas, were synthesized in this experiment. The preparation method followed the procedure reported by Ibrahim et al. (2013, 2015). Briefly, an aqueous solution of $Ca(NO_3)_2$ and H_3PO_4 was prepared at a molar ratio of 5 to 3. The pH of the $Ca(NO_3)_2$ solution was adjusted to 10.5 by the addition of 0.1 mol/L NaOH solution. H_3PO_4 was added at a controlled rate into the $Ca(NO_3)_2$ solution with a syringe pump (TCI-IV, RunLian, Hebei, China), and reacted at room temperature under vigorous agitation at 450 r/min for 30 min. Two addition rates (25 and 200 mL/hr) of H_3PO_4 were used to control the surface area of HAP. Finally, the products were filtered, washed with deionized water and ethanol, and then freeze–dried.

1.2. Characterization of the HAP samples

The basic properties of the HAP samples were determined as follows. The phase structures of the HAP samples were analyzed by X-ray diffraction (XRD, X'Pert, Philips, Amsterdam, Netherlands). The N_2 adsorption–desorption isotherms were determined using a surface area analyzer (Ommishop 100cx, Beckman Coulter Inc., Brea, CA, USA). The morphology and microstructure were observed using scanning electron microscopy (SEM: SU8020, Hitachi, Chiyoda, Japan). The SEM was equipped with an ISIS 310 energy dispersive spectrometer (EDS) system (Aztec X-Max 80, Oxford, UK).

1.3. Sorption kinetics and isotherm experiments

For the sorption kinetic experiments, exactly 0.1 g of LHAP or SHAP was added to 30-mL of a solution containing 3 mmol/L Cd and/or Pb solution in a 50-mL centrifuge tube. The samples were agitated in a horizontal shaker at 200 r/min at 25 ± 2°C. The supernatants were separated by centrifugation at 6000 r/min for 5 min, and filtered through 0.45-μm polypropylene membrane filters. Filtrates were collected to measure the concentrations of Cd and Pb. In addition to the solution analysis, the reaction products were also collected at the end of reaction, freeze-dried, and then used for XRD and SEM-EDS analyses.

For the isotherm experiments, the concentrations of Cd and Pb added varied from 1 to 8 mmol/L. In the binary-metal systems, one metal was kept at 3 mmol/L. The quantity of sorbed Cd/Pb was calculated by the difference in the concentration before and after the sorption experiment. All samples were incubated for 7 days to reach sorption equilibrium.

The initial and final pH values for the solutions of LHAP with different initial metal concentrations ranged from 6.73 to 5.78 for Cd, and from 6.85 to 6.74 for Pb, respectively. The

corresponding values for SHAP ranged from 6.57 to 5.53 for Cd, and from 6.81 to 6.69 for Pb, respectively. In these suspensions, the initial ph and final pH were measured but not adjusted.

1.4. Computation and model

The amount of Cd and Pb removed from the solutions per gram of HAP was calculated using the equation:

$$Q = (C_0 - C_e) \times V/M \quad (1)$$

where, Q (mmol/g) is the Cd and Pb loading onto HAP, C_0 (mmol/L) denotes the concentration of Cd and Pb in the solution before mixing with HAP, C_e (mmol/L) is the equilibrium concentration of Cd and Pb remaining in the solution after the sorption experiment, V (L) is the volume of the solution, and M (g) denotes the mass of HAP. A quantitative analysis of the Cd and Pb concentrations was performed using inductively coupled plasma (ICP) and inductively coupled plasma-mass spectrometry (ICP-MS).

First- and second-order models were used to simulate the sorption kinetics data. The equations for these models can be written as:

$$\text{First–order}: Q_t = Q_e\left(1 - e^{-k_1 t}\right) \quad (2)$$

$$\text{Second–order}: Q_t = \frac{k_2 Q_e^2 t}{1 + k_2 Q_e t} \quad (3)$$

where, Q_t (mmol/g) and Q_e (mmol/g) are the amount of Cd and Pb adsorbed on the HAP at time t and reaction equilibrium, respectively, and k_1 (hr^{-1}) and k_2 (hr^{-1}) are the first- and second-order sorption rate constants, respectively.

The Langmuir and Freundlich models were used to simulate the sorption isotherms. The equations can be written as:

$$\text{Langmuir}: Q = \frac{k_L Q_m C_e}{1 + kC_e} \quad (4)$$

$$\text{Freundlich}: Q = k_F C_e^{1/n} \quad (5)$$

where, k_L (L/mmol) is the Langmuir constant related to bonding energies, k_F ($(mmol^{(1-n)} \cdot L^n)/g$) is the Freundlich affinity coefficient, Q_m (mmol/g) is the Langmuir maximum capacity, C_e (mmol/g) is the equilibrium solution concentration of each metal in solution, and n is the Freundlich linearity constant.

1.5. Soil preparation

Uncontaminated soils used for maize cultivation were collected at a depth of 0–20 cm from Tongcheng County, Auqing City, China (31°07′N, 116°53′E). The soil samples were air-dried and ground to pass through a 60-mesh sieve. Selected properties of the investigated soil are as following: pH 6.30, soil organic matter 12.3 g/kg, cation exchange capacity 12.6 cmol/kg, clay 21.8%, total Cd concentration 0.17 mg/kg, and total Pb concentration 29.8 mg/kg.

To simulate the levels of Cd and Pb pollution, the soil samples were placed in polythene pots. The soils were mixed with single- and mixed-metal solutions of $Cd(NO_3)_2$ and $Pb(NO_3)_2$ at a concentration of 1 mmol/kg respectively, and incubated at constant humidity (70% water holding capacity) for one month at 25°C. The pots were then covered by a plastic lid containing several small holes to allow gaseous exchange and minimize moisture loss. After one month, the two HAP materials were mixed with 100 g of contaminated soil at rates of 3.0% by weight in 500-mL plastic beakers, respectively. The HAPs were thoroughly mixed with the soils to obtain homogeneity. All the beakers were covered with a plastic film to prevent moisture loss and then incubated at a constant temperature of 25°C for 60 days. At day 60, European Community Bureau of Reference (BCR) sequential extraction tests of the soil samples were conducted.

1.6. Cd and Pb species in the soil

To determine the changes in Cd and Pb speciation in soils before and after amendment with HAPs, the BCR sequential extraction method was applied to quantify the fractions of various defined Cd and Pb species (Quevauviller et al., 1993; Alborés et al., 2000). The Cd and Pb speciation in the soil was classified into acid-soluble metals, reducible metals, oxidizable metals, and residual metals. The acid-soluble metals were extracted by acetic acid; the Pb and Cd bound with Fe/Mn oxides (the reducible metals) were analyzed using hydroxylamine hydrochloride; the Pb and Cd combined with organic matter and sulfides (the oxidizable metals) were determined using H_2O_2 and NH_4OAc; and the residual fraction was digested with HNO_3–HF–$HClO_4$. For each step, the equivalent of 0.50 g dry weight of extractant was added to the soil sample in a 50-mL centrifuge tube. The soil samples included both unamended and amended soils. The suspensions were subsequently shaken for 16 hr to reach reaction equilibrium, and the solution phase of the suspensions was then separated from the solid phase by centrifugation at 10,000 r/min for 10 min. The supernatants were decanted and filtered through a 0.22-μm pore-size Millipore filter. The filtrates were stored at 4°C prior to analysis for Cd and Pb, whereas the soil residues were retained for the next step. The same centrifugation–decantation procedure was used for each extraction.

1.7. Data analysis

The data were analyzed using the SPSS 16.0 statistical package and Excel 2007 for Windows. The means of three replicates were subjected to a one-way analysis of variance and the Tukey honest significant difference test at the 0.05 significance level.

2. Results and discussion

2.1. Characterization of HAP samples

Fig. 1 shows SEM images of the two HAP samples, with different structures and morphologies. The SHAP has an irregular, blocky structure, with a particle size of about 1–5 μm (Fig. 1a). The image of LHAP shows that a large quantity of hydroxyapatite nanosheets formed on the surface and became integrated into the micro-structure (Fig. 1b). The

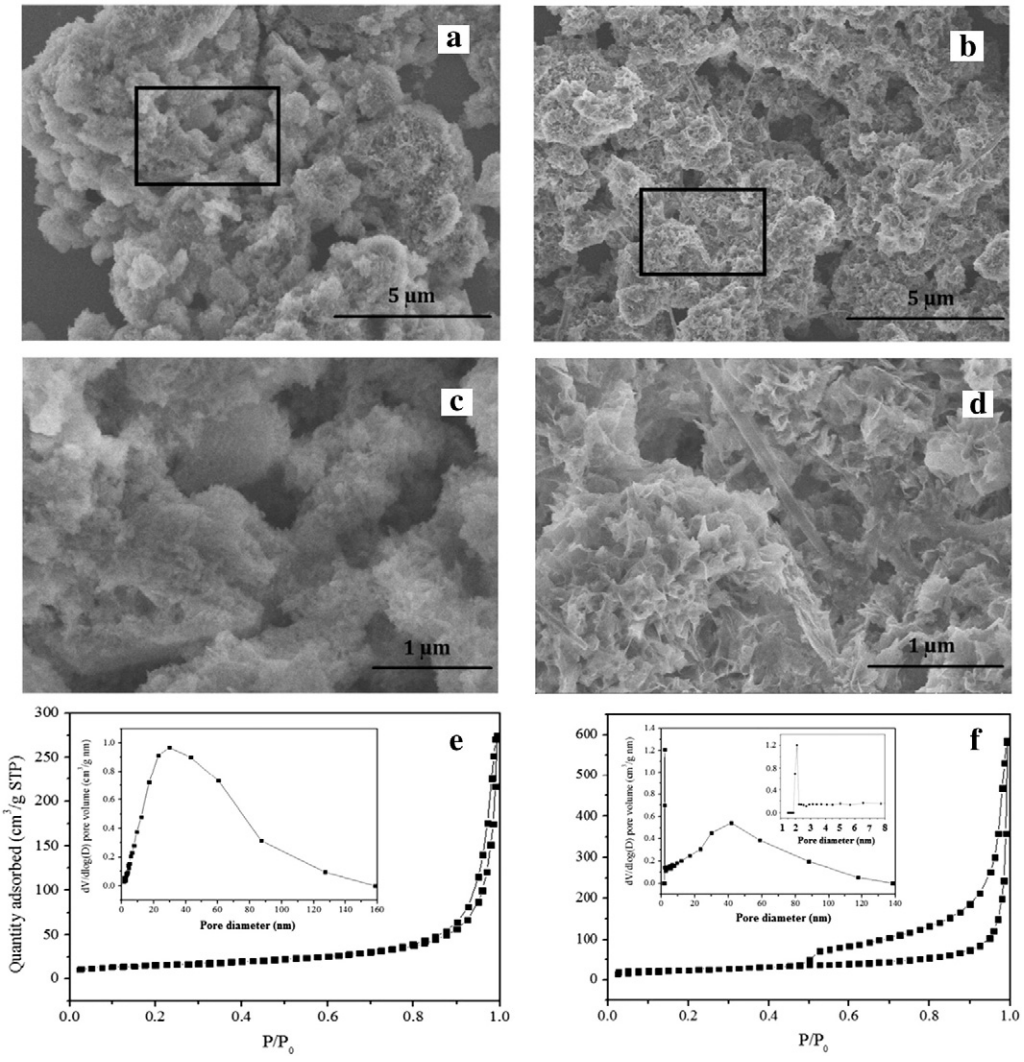

Fig. 1 – Scanning electron microscopy (SEM) images of non-reacted samples of small surface area hydroxyapatite (SHAP) (a) and large surface area hydroxyapatite (LHAP) (b) and magnified regions of a (c) and b (d). Nitrogen adsorption–desorption isotherms and pore size distribution curve (inset) of SHAP (e) and LHAP (f). Standard temperature and pressure (STP): the monolayer area was paved by per milliliter of N_2 molecule; P/P0: relative pressure.

surface of LHAP was also rougher than that of SHAP (Fig. 1c and d). The XRD pattern in Fig. 2 shows that the diffraction peaks of the LHAP and SHAP were in agreement with those of the Joint Committee on Powder Diffraction Standards (JCPDS) card No. 09–0432, which confirmed the as-prepared products were HAP samples (Ibrahim et al., 2013).

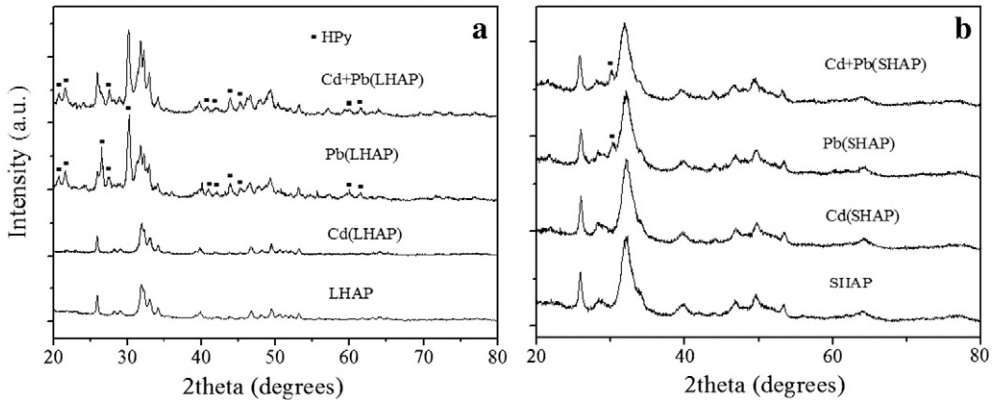

Fig. 2 – X-ray diffraction (XRD) patterns of LHAP (a) and SHAP (b) before and after reaction with Cd or/and Pb solutions.

For further insight into the surface area and pore-size distribution of the two HAP samples, the N_2 adsorption–desorption isotherms were measured to examine the structural characteristics of the pores (Fig. 1e and f). The surface area and pore volume of LHAP, calculated from the nitrogen sorption isotherms, was 187.16 m^2/g and 0.89 cm^3/g (Table 1), which was larger than the corresponding values of 46.79 m^2/g and 0.37 cm^3/g for SHAP, respectively. From the corresponding pore size distribution curves (inset in Fig. 1e and f), we found an obvious difference in the pore size distribution for the two HAP samples. The pore size of SHAP was widely distributed, with a peak of around 30 nm (inset in Fig. 1e). However, there were two peak sizes found in the pore structure of LHAP (inset in Fig. 1f). One was distributed around 2 nm and the other was centered around 42 nm. The peak around 2 nm was derived from the close arrangement of the nanosheets on the surface of LHAP, and the larger pores were mainly attributed to the loose accumulation of bulk LHAP, which was similar to the pores of SHAP. The results indicated that the dispersed nanosheets led to the formation of the small nanopores in the LHAP structure and the large specific area that was obtained.

2.2. Sorption kinetics of Cd and Pb

The sorption kinetics of Cd and Pb by LHAP and SHAP in single- and binary-metal solutions was examined (Fig. 3). The kinetic models described the experimental data fairly well, with all R^2 values being greater than 0.85 in single-metal systems (Table 2). The estimated Q_e of the metal concentration for LHAP and SHAP in the single system using the models (Table 2) was consistent with the observed value (see Fig. 3a). However, for the binary-metal system, the first-order model did not fit the model better than the second-order model. Moreover, the Q_e of Cd and Pb for LHAP in the binary system estimated by the first-order model was 0.18 and 0.52 mmol/g (Table 2), which is about 14% and 21% less than the observed value (0.21 and 0.66 mmol/g, see Fig. 3b). Thus, the second-order model performed better for both LHAP and SHAP in single- and binary-metal systems. The best-fit kinetic model parameters are presented in Table 2.

Q_e values were different in the binary-metal system using the two HAP materials according to the second-order model (Table 2). For Cd treatment, the Q_e of both LHAP (0.69 mmol/g) and SHAP (0.34 mmol/g) was higher in a single-metal solution than in the binary-metal system (0.21 mmol/g for LHAP and 0.19 mmol/g for SHAP), which was identical to the trend in Pb treatment. These data indicated competitive sorption between Cd and Pb on HAP in the binary-metal system. The Q_e of the LHAP in the Cd-only system was about 2.1 times higher than the Q_e of the SHAP. However, the presence of Pb can decrease the variation of Cd and Pb adsorbed on LHAP and SHAP. For example, the difference in Q_e for Cd between LHAP and SHAP was 10% in the binary system, and the corresponding values of Pb were 3.8% and 3% in the single- and binary-metal systems, respectively. The results indicated that Pb had an inhibitive effect on the Cd and Pb sorption capacity of LHAP in the single- and binary-metal system, compared with SHAP. This might be explained by the different reaction mechanisms of HAP with Cd and Pb. Surface complexation is the main sorption mechanism for Cd (Smičiklas et al., 2000; Mobasherpour et al., 2011), while Pb could form a hydroxypyromorphite (HPy) precipitate through the dissolution–precipitation mechanism (Cao et al., 2004).

Table 1 – Physical properties of two hydroxyapatite (HAP) materials and large surface area hydroxyapatite loaded with Cd or/and Pb.

Sample	Specific surface area (m^2/g)	Pore volume (cm^3/g)	Average pore diameter (nm)
LHAP	187.16	0.89	2.09
SHAP	46.79	0.37	25.93
LHAP with Cd	177.42	0.78	2.23
LHAP with Pb	237.60	0.23	12.12
LHAP with Cd and Pb	89.30	0.12	17.19

2.3. Sorption isotherm of Cd and Pb

Cd and Pb sorption by HAP was analyzed using the Langmuir and Freundlich models. Although both models reproduced the isotherm data very well, the Langmuir model ($R^2 > 0.95$) fitted the HAP sorption isotherm better than the Freundlich model ($0.80 < R^2 < 0.90$) (Table 2). Generally, the Langmuir model assumes monolayer adsorption onto a homogeneous surface with no interactions between the adsorbed molecules, while the Freundlich model is an empirical equation commonly used for heterogeneous surfaces. Synthetic HAP is a pure substance without impurities, so the adsorption surface of HAP is considered to be homogeneous. In the previous study by Zhang et al. (2010), the XPS analysis revealed that Cd and Pb sorption might only have occurred on the outer surfaces of HAP, as Cd and Pb signals were not detected 10 nm below the surface. The heavy metals were adsorbed on the outer surface of HAP, which is appropriate for monolayer adsorption. Thus, the Langmuir model was more suitable for the surface homogeneity of HAP. Previous studies have reported that the Langmuir model describes the sorption process of heavy metals on hydroxyapatite well (Xu et al., 1994; Cao et al., 2004; Baillez et al., 2007; Corami et al., 2008). The best-fit isotherm model parameters are listed in the supporting information (Table 2).

In the Cd-only system, the plateau of the LHAP isotherm was three times higher than that of the SHAP isotherm; however, there was no significant variation ($p < 0.05$) between the LHAP and SHAP isotherms when Pb was added (Fig. 4). The Q_m of Cd/Pb in single-metal and binary systems was compared with the values between LHAP and SHAP though the Langmuir model. The Q_m of LHAP (1.85 mmol/g) for Cd in the single-metal system was higher than the Q_m of SHAP (0.64 mmol/g). Previous studies have shown that the sorption capacity of Cd rises as the surface area of HAP increases (Zhang et al., 2010). Da Rocha et al. (2002) found that the maximum sorption capacity normalized to specific surface area could be almost constant for any HAP. Thus, LHAP displayed a higher sorption capacity than SHAP for Cd adsorption due to its high surface area. However, the Q_m of Cd for LHAP was only 12% higher than SHAP in the binary-metal solution. The Q_m of Pb was less different (3.2%

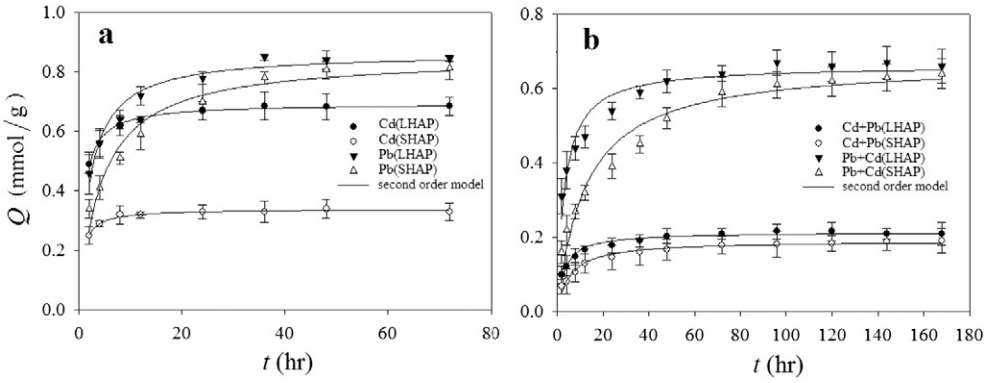

Fig. 3 – Sorption kinetics of single-metal solution (a) and binary-metal solution (b) by LHAP and SHAP respectively, showing the amount of adsorbed Cd and Pb (Q) versus time. Initial Cd and Pb = 3 mmol/L, amount of HAP = 0.1 g and Temperature = 25 ± 2°C. Cd: the amount of adsorbed Cd in single-Cd solution, Pb: the amount of adsorbed Pb in single-Pb solution, Cd + Pb: the amount of adsorbed Cd in binary-metal solution, Pb + Cd: the amount of adsorbed Pb in binary-metal solution.

for a single-metal system and 2% for a binary system) between the LHAP and SHAP (Table 2). These results suggest that the effect of surface area on the adsorption capacity of Cd and Pb by LHAP was low due to the presence of Pb, which is in agreement with previous studies (Peld et al., 2004).

2.4. *The sorption mechanism for Cd and Pb*

The LHAP's morphology and structure might also explain the sorption variations observed in the presence of Pb. To confirm the sorption process of Cd and Pb by the LHAP and SHAP, SEM observations with EDS analysis and XRD measurements were performed on the HAP sample after the experiments with the single- and binary-metal solutions (Fig. 5).

For the LHAP reaction with Cd, the SEM results showed that the overall morphology of the LHAP was consistent with that of the original sample before the experiments (Fig. 5a). The X-ray diffraction patterns of LHAP did not indicate any modification in the crystalline phase after the adsorption experiments (Fig. 2a). However, the presence of Cd^{2+} ions in the LHAP structure was confirmed by EDS (Fig. 5b). Therefore, dissolution–precipitation was not the main Cd sorption mechanism for the LHAP. Some studies have reported that the reaction of Cd^{2+} with hydroxyapatite may not proceed through a dissolution–precipitation mechanism that results in the formation of a precipitate (Zheng et al., 2007; Silvano et al., 2012). Compared with the original HAP, there was less variation in the specific area, pore volume, and average pore diameter of LHAP after the experiments with the Cd-only solution (Table 1), suggesting that the channel structure remained in place. Generally, the sorption process of Cd includes two steps: surface complexation and ion exchange followed by the diffusion of Cd into the structure of HAP (Fedoroff et al., 1999; Marchat et al., 2007). The stable structure and intact morphology of LHAP promoted the accessibility of Cd to reactive sites even after it reacted with Cd, and thus the larger specific surface area enhanced Cd adsorption by LHAP.

For LHAP reacted with Pb, the SEM images indicated an alteration of morphology and the dissolution of the HAP surface, while EDS detected a large amount of Pb^{2+} in the LHAP phase (Fig. 5c and d). The coexistence of the HAP and HPy phases was observed (Fig. 6a and b), indicating the occurrence of the dissolution–precipitation reaction in Pb adsorption by LHAP. Additional peaks were detected by XRD and identified as HPy in the LHAP residue after its reaction with Pb (Fig. 2a), which further confirmed that a HPy precipitate formed due to the reaction between Pb and LHAP. After the LHAP was loaded with Pb, the pore volume of the product decreased, but the specific surface area increased (Table 1). The increase in the surface area was due to the

Table 2 – Best-fit model parameters of Cd and Pb sorption in single- and binary-metal system by LHAP and small surface area hydroxyapatite (SHAP).

System	Treatment	First-order			Second-order			Langmuir			Freundlich		
		k_1	Q_e	R^2	k_2	Q_e	R^2	k_L	Q_m	R^2	k_F	n	R^2
Single-metal	Cd(LHAP)	0.59	0.66	0.87	1.64	0.69	0.99	1.59	1.85	1.00	1.04	3.25	0.98
	Cd(SHAP)	0.67	0.33	0.91	4.28	0.34	0.98	2.37	0.64	0.99	0.43	3.16	0.98
	Pb(LHAP)	0.31	0.80	0.86	0.55	0.86	0.96	18.07	1.96	0.99	1.68	7.40	0.93
	Pb(SHAP)	0.17	0.77	0.87	0.27	0.85	0.96	11.46	1.90	0.99	1.46	5.87	0.91
Binary-metal	Cd (LHAP)	0.22	0.18	0.80	1.57	0.21	0.97	1.86	0.47	0.98	0.29	3.28	0.94
	Cd (SHAP)	0.13	0.18	0.84	0.95	0.19	0.97	1.47	0.42	0.97	0.24	3.08	0.92
	Pb (LHAP)	0.20	0.52	0.75	0.46	0.66	0.94	6.21	1.73	1.00	1.32	5.34	0.94
	Pb (SHAP)	0.06	0.60	0.83	0.12	0.67	0.96	3.10	1.69	0.99	1.18	4.23	0.93

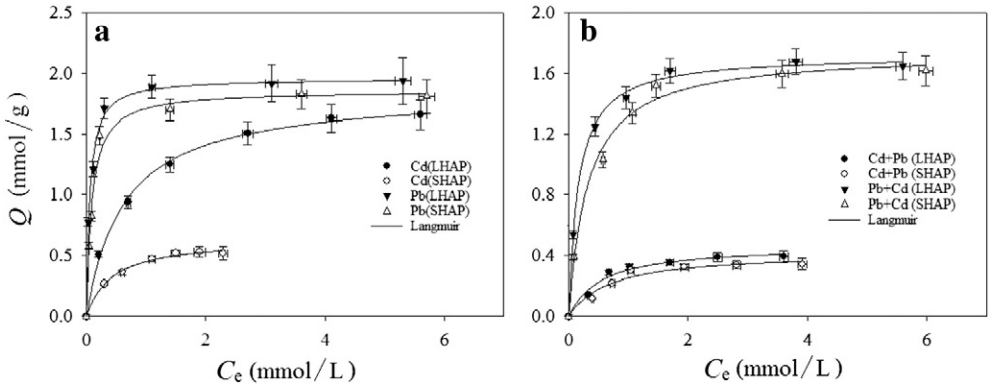

Fig. 4 – Isotherm of single-metal solution (a) and binary-metal solution (b) sorption on LHAP and SHAP, respectively. Cd: the amount of adsorbed Cd in single-Cd solution, Pb: the amount of adsorbed Pb in single-Pb solution, Cd + Pb: the amount of adsorbed Cd in binary-metal solution, Pb + Cd: the amount of adsorbed Pb in binary-metal solution.

newly formed rod-like precipitates. Similar changes were apparent in the morphology of LHAP loaded with Pb and Cd (Fig. 5e). The LHAP surface was partially dissolved and the small nanosheets became larger, with rod-like precipitates observed on the surface (Fig. 6c). After the impurities were formed and covered the surface of LHAP due to the formation

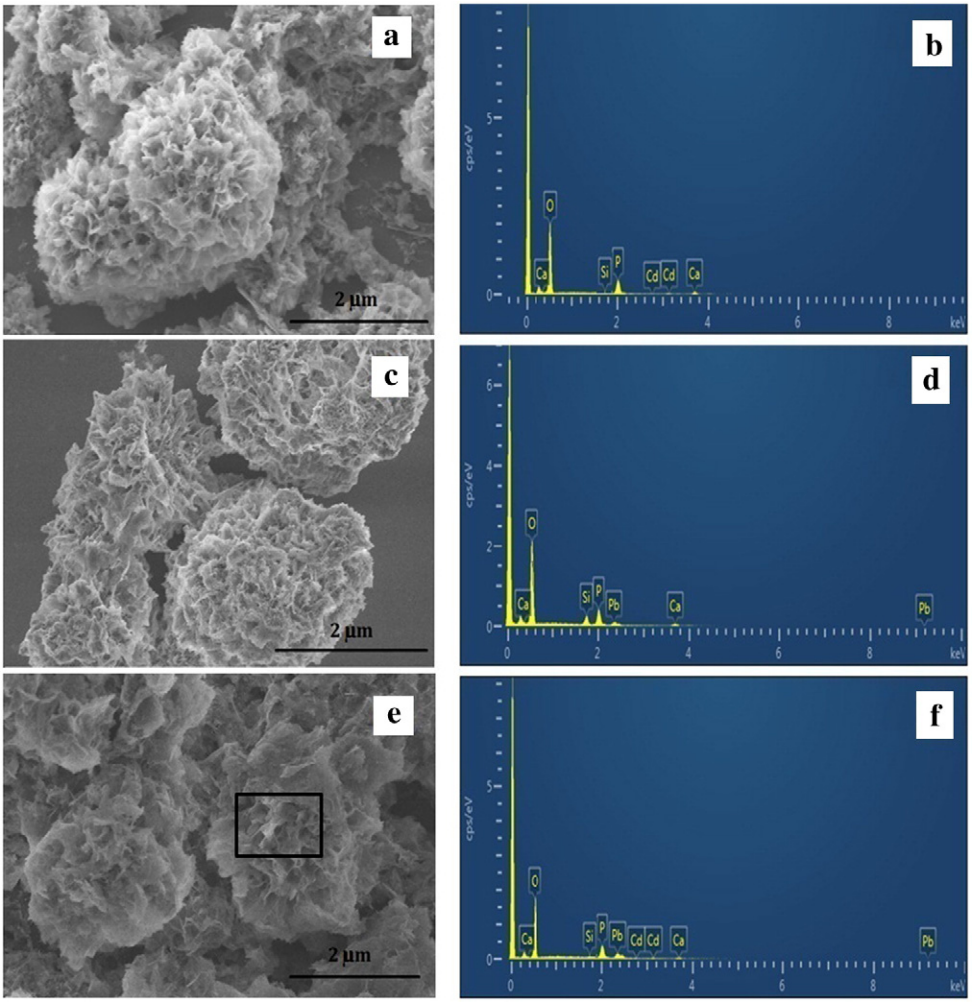

Fig. 5 – SEM images and energy dispersive spectrometer (EDS) spectra of the reacted samples of LHAP with Cd (a and b), Pb (c and d) and Cd + Pb (e and f) solutions.

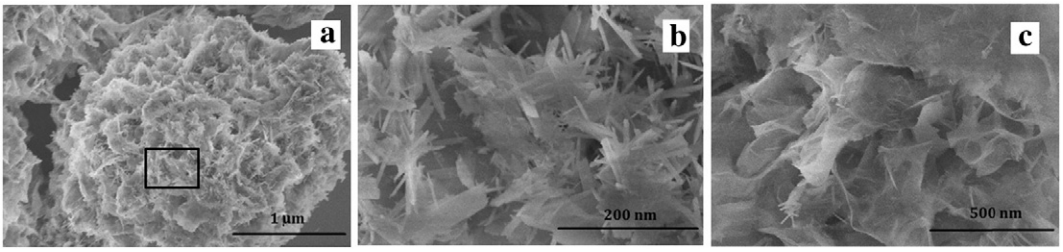

Fig. 6 – SEM images of HAP after reaction with solutions containing heavy metals. (a) Was the magnified image in Fig. 5c, and (b) is the magnifications of the area delimited by the square in panel a. (c) was the magnifications of the area delimited by the squares in Fig. 5e.

of HPy, the original small holes and channels were blocked in the LHAP structure, which decreased the specific surface area and pore volume of LHAP (Table 1). Irani et al. (2011) reported that the formation of impurities on the surface of an amendment can lead to metal ions being weakly diffused into the pores on the internal surface, decreasing the sorption capacity for Pb ions. Strong Cd and Pb signals were detected on the surface of LHAP in the EDS spectrum, showing that Cd and Pb associated with Ca, P, and O, which are immobilized on the surface of LHAP (Fig. 5f). These results indicated that the dissolution of the surface structure and the blockage of channels can reduce metal ion diffusion into the inner framework of the LHAP, and the sorption capacity of LHAP for Cd and Pb was then decreased after it reacted with Pb.

2.5. *Fractions of Cd and Pb extracted when 1.0 mmol/kg of the heavy metals were added to the soil*

We verified the conclusions obtained in the experiment on the removal of Cd and Pb from solution using LHAP and SHAP, though the remediation of single- and binary-metal contaminated soil. Accordingly, Cd and Pb partitioning occurred in soil samples treated with the two HAP samples (Table 3). The acid-soluble fractions of Cd and Pb extracted by 0.11 mol/L acetic acid primarily consisted of soluble, exchangeable, and carbonate-combined heavy metals (Quevauviller et al., 1994). This fraction represents the active and bioavailable metal speciation. As shown in Table 3, the two types of HAP significantly reduced the acid-soluble concentrations of Cd and Pb in the soil. Specifically, the acid-soluble Cd decreased by 43% and 24% in single-metal soil, and 22% and 18% in binary-metal soil the for LHAP and SHAP treatments, respectively. The corresponding values for Pb were 87% and 85% in single-metal soil, and 67% and 63% in binary-metal soil for the LHAP and SHAP treatments, respectively. A significant difference ($p < 0.05$) in the acid-soluble Cd levels was observed between the LHAP and SHAP treatment in single Cd contaminated soil, which suggested that the large specific area could facilitate the immobilization of Cd in the single-metal contaminated soil. However, there was no significant variation in the acid-soluble metal levels between the LHAP and SHAP treatments when the soils were spiked with Pb. Therefore, large surface area HAP will enhance the remediation of a soil that is polluted only with Cd, but not a soil polluted with Pb or both Pb and Cd, which is consistent with the results of the LHAP and SHAP tests with the single- and binary-metal solutions.

The acid-soluble Cd reduced by LHAP and SHAP was primarily transformed to the reducible and oxidizable forms (Table 3). Compared with the treatment with no added HAP, the reducible portion in soil contaminated by Cd alone increased by 2.7 and 1.9 times in response to treatment with

Table 3 – Fraction of Cd and Pb determined by European Community Bureau of Reference (BCR) sequential extraction for the treatments with 1.0 mmol/kg of metals (unit: mmol/kg).

Metal	Treatment	Acid soluble metals	Reducible metals	Oxidizable metals	Residual metals
Cd (single-metal)	CK	0.68 ± 0.034a	0.12 ± 0.010 c	0.06 ± 0.006 c	0.13 ± 0.011 a
	LHAP	0.39 ± 0.023c	0.33 ± 0.023a	0.13 ± 0.005a	0.14 ± 0.009a
	SHAP	0.52 ± 0.018b	0.23 ± 0.028b	0.09 ± 0.007b	0.15 ± 0.013a
Cd (binary-metal)	CK	0.63 ± 0.032a	0.13 ± 0.01b	0.05 ± 0.007b	0.14 ± 0.006b
	LHAP	0.49 ± 0.015b	0.20 ± 0.01a	0.13 ± 0.006a	0.17 ± 0.006a
	SHAP	0.52 ± 0.042ab	0.21 ± 0.018a	0.13 ± 0.007a	0.15 ± 0.008a
Pb (single-metal)	CK	0.57 ± 0.036a	0.15 ± 0.005b	0.06 ± 0.007b	0.23 ± 0.015b
	LHAP	0.07 ± 0.012b	0.31 ± 0.026a	0.17 ± 0.011a	0.49 ± 0.031a
	SHAP	0.09 ± 0.010b	0.34 ± 0.034a	0.16 ± 0.006a	0.46 ± 0.027a
Pb (binary-metal)	CK	0.51 ± 0.046 a	0.17 ± 0.006b	0.05 ± 0.004b	0.25 ± 0.018b
	LHAP	0.13 ± 0.010b	0.30 ± 0.018a	0.14 ± 0.023a	0.45 ± 0.026a
	SHAP	0.15 ± 0.016b	0.29 ± 0.026a	0.11 ± 0.013a	0.42 ± 0.037a

Means ($n = 3$) followed by same letter within a column are not significantly different ($p > 0.05$). CK: control treatment.

LHAP and SHAP, while the oxidizable Cd increased by 2.4 and 1.6 times, respectively. The corresponding values in the binary-metal system increased by 1.5 and 1.6 times for the LHAP and SHAP treatment, and 2.4 and 2.5 times for the LHAP and SHAP treatment, respectively. This transformation was primarily attributed to the strong surface complexation and ion exchange with metals by HAP (Ma et al., 2010; Cui et al., 2013). LHAP could increase the portion of reducible and oxidizable Cd more than that of SHAP in the Cd-only contaminated soil, but not in binary-metal contaminated soils. The concentration of reducible Cd declined in the LHAP treatment as the Pb entered into the soil. The reason was that Pb in soil could react with LHAP, and lead to damage of the original small holes and channels in the LHAP structure, which decreased the active sites of LHAP and reduced the ability of HAP for surface complexation and ion exchange with heavy metals. The content of residual Cd changed only slightly when the two HAP samples were incorporated, because the precipitation reaction was not the main Cd immobilization mechanism for HAP, and did not lead to an obvious change in the residual portion of Cd (Cui et al., 2013).

In addition to the reducible and oxidizable forms, the acid-soluble Pb was significantly converted ($p < 0.05$) to residual forms of Pb due to the formation of pyromorphite. Similar results were also observed by Ryan et al. (2001) and Melamed et al. (2003), who found that phosphate treatments resulted in a significant shift of active Pb to residual Pb due to the production of HPy, which was confirmed by extended X-ray absorption fine structure spectroscopy (Hashimoto et al., 2009). In the Pb-contaminated soils, the three metal fractions in the LHAP treatment did not increase more significantly than in the SHAP treatment. The results indicate that LHAP has the potential to improve the immobilization of Cd-only polluted soils, but is useless for enhancing the remediation of contaminated soil when Pb is also present.

3. Conclusions

The sorption kinetics and isotherms of Cd and Pb on LHAP and SHAP could be modeled by the second order kinetics model and Langmuir isotherm. LHAP showed higher adsorption capacity for Cd than SHAP due to its high surface area. Competitive sorption occurred in the binary systems, and Pb exhibited a greater inhibition effect on the sorption of heavy metal for LHAP than that for SHAP. The significant differences between the sorption dynamic curves and Q_m suggested possible differences in the specific mechanisms for metal sorption between LHAP and SHAP. The results of XRD, SEM-EDS and N_2 adsorption–desorption isotherms indicated that the mechanism of HAP dissolution following HPy precipitation was dominant and led to a loss in the porosity and a decrease in the number of effective reactive sites, which can strongly influence the sorption capacity of LHAP. Sequential extraction analysis indicated that the addition of Pb significantly decreased the immobilization efficiency of LHAP for heavy metals. Therefore, the reduced efficiency of LHAP due to the role of Pb ions should be carefully considered for practical environmental applications in the treatment of wastewater and soil containing heavy metals.

Acknowledgments

This research was supported by the National Natural Science Foundation of China (No. 41301347), the Anhui Provincial Natural Science Foundation (No. 1408085MKL61), the Scientific and Technical Key Research Program of Auhui (No. 1501031088), and the Natural Science Foundation of Anhui Academy of Agricultural Sciences (No. 16A1029).

REFERENCES

Alborés, A.F., Cid, B.P., Gómez, E.F., López, E.F., 2000. Comparison between sequential extraction procedures and single extractions for metal partitioning in sewage sludge samples. Analyst 125 (7), 1353–1357.

Baillez, S., Nzihou, A., Bernache-Assolant, D., Champion, E., Sharrock, P., 2007. Removal of aqueous lead ions by hydroxyapatites: equilibria and kinetic processes. J. Hazard. Mater. 139 (3), 443–446.

Cao, X.D., Ma, L.Q., Rhue, D.R., Appel, C.S., 2004. Mechanisms of lead, copper, and zinc retention by phosphate rock. Environ. Pollut. 131 (3), 435–444.

Christoffersen, J., Christoffersen, M.R., Larsen, R., Rostrup, E., Tingsgaard, P., Andersen, O., Grandjean, P., 1988. Interaction of cadmium ions with calcium hydroxyapatite crystals: a possible mechanism contributing to the pathogenesis of cadmium-induced bone diseases. Calcif. Tissue Int. 42 (5), 331–339.

Corami, A., Mignardi, S., Ferrini, V., 2008. Cadmium removal from single- and multi-metal (Cd + Pb + Zn + Cu) solutions by sorption on hydroxyapatite. J. Colloid Interface Sci. 317 (2), 402–408.

Cui, H.B., Zhou, J., Zhao, Q.G., Si, Y.B., Mao, J.D., Fang, G.D., Liang, J.N., 2013. Fractions of Cu, Cd, and enzyme activities in a contaminated soil as affected by applications of micro- and nanohydroxyapatite. J. Soils Sediments 13 (4), 742–752.

Da Rocha, N.C.C., De Campos, R.C., Rossi, A.M., Moreira, E.L., Barbosa, A.D., Moure, G.T., 2002. Cadmium uptake by hydroxyapatite synthesized in different conditions and submitted to thermal treatment. Environ. Sci. Technol. 36 (7), 1630–1635.

Fedoroff, M., Jeanjean, J., Rouchaud, J.C., Mazerolles, L., Trocellier, P., Maireles-Torres, P., Jones, D.J., 1999. Sorption kinetics and diffusion of cadmium in calcium hydroxyapatites. Solid State Sci. 30 (47), 71–83.

Gray, C.W., Dunham, S.J., Dennis, P.G., Zhao, F.J., McGrath, S.P., 2006. Field evaluation of in situ remediation of a heavy metal contaminated soil using lime and red-mud. Environ. Pollut. 142 (3), 530–539.

Hashimoto, Y., Takaoka, M., Oshita, K., Tanida, H., 2009. Incomplete transformations of Pb to pyromorphite by phosphate-induced immobilization investigated by X-ray absorption fine structure (XAFS) spectroscopy. Chemosphere 76 (5), 616–622.

Ibrahim, A., Wei, W.X., Zhang, D., Wang, H.T., Li, J., 2013. Conversion of waste eggshells to mesoporous hydroxyapatite nanoparticles with high surface area. Mater. Lett. 110 (11), 195–197.

Ibrahim, A., Zhou, Y.L., Li, X.Y., Chen, L., Hong, Y.Z., Su, Y.Z., Wang, H.T., Li, J., 2015. Synthesis of rod-like hydroxyapatite with high surface area and pore volume from eggshells for effective adsorption of aqueous Pb(II). Mater. Res. Bull. 62, 132–141.

Irani, M., Amjadi, M., Mousavian, M.A., 2011. Comparative study of lead sorption onto natural perlite, dolomite and diatomite. Chem. Eng. J. 178 (24), 317–323.

Jang, S.H., Min, B.G., Jeong, Y.G., Lyoo, W.S., Lee, S.C., 2008. Removal of lead ions in aqueous solution by hydroxyapatite/polyurethane composite foams. J. Hazard. Mater. 152 (3), 1285–1292.

Lee, S.H., Lee, J.S., Choi, Y.J., Kim, J.G., 2009. In situ stabilization of cadmium-, lead-, and zinc-contaminated soil using various amendments. Chemosphere 77 (8), 1069–1075.

Leyva, A.G., Marrero, J., Smichowski, P., Cicerone, D., 2001. Sorption of antimony onto hydroxyapatite. Environ. Sci. Technol. 35 (18), 3669–3675.

Lusvardi, G., Malavasi, G., Menabue, L., Saladini, M., 2002. Removal of cadmium ions by means of synthetic hydroxyapatite. Waste Manag. 22 (8), 853–857.

Ma, L., Xu, R.K., Jiang, J., 2010. Adsorption and desorption of Cu(II) and Pb(II) in paddy soils cultivated for various years in the subtropical China. J. Environ. Sci. 22 (5), 689–695.

Mandjiny, S., Matis, K., Zouboulis, A., 1998. Calcium hydroxyapatites: evaluation of sorption properties for cadmium ions in aqueous solution. J. Mater. Sci. 33 (22), 5433–5439.

Mandjiny, S., Zouboulis, A.I., Matis, K.A., 1995. Removal of cadmium from dilute solutions by hydroxyapatite. I. Sorption studies. Sep. Purif. Technol. 30 (15), 2963–2978.

Marchat, D., Bernache-Assollant, D., Champion, E., 2007. Cadmium fixation by synthetic hydroxyapatite in aqueous solution-thermal behavior. J. Hazard. Mater. 139 (3), 453–460.

Melamed, R., Cao, X.D., Chen, M., Ma, L.Q., 2003. Field assessment of lead immobilization in a contaminated soil after phosphate application. Sci. Total Environ. 305 (1–3), 117–127.

Mobasherpour, I., Salahi, E., Pazouki, M., 2011. Removal of divalent cadmium cations by means of synthetic nano crystallite hydroxyapatite. Desalination 266 (s 1–3), 142–148.

Peld, M., Tonsuaadu, K., Bender, W., 2004. Sorption and desorption of Cd^{2+} and Zn^{2+} ions in apatite-aqueous systems. Environ. Sci. Technol. 38 (21), 5626–5631.

Quevauviller, P., Rauret, G., Griepink, B., 1993. Single and sequential extraction in sediments and soils. Int. J. Environ. Anal. Chem. 51 (1–4), 231–235.

Quevauviller, P., Rauret, G., Muntau, H., Ure, A.M., Rubio, R., Lopezsanchez, J.F., Fiedler, H.D., Griepink, B., 1994. Evaluation of a sequential extraction procedure for the determination of extractable trace metal contents in sediments. Fresenius J. Anal. Chem. 349 (12), 808–814.

Ryan, J.A., Zhang, P., Hesterberg, D., Chou, J., Sayers, D.E., 2001. Formation of chloropyromorphite in a lead-contaminated soil amended with hydroxyapatite. Environ. Sci. Technol. 35 (18), 3798–3803.

Sandrine, B., Ange, N., Didier, B.A., Eric, C., Patrick, S., 2007. Removal of aqueous lead ions by hydroxyapatites: equilibria and kinetic processes. J. Hazard. Mater. A139 (3), 443–446.

Seaman, J.C., Arey, J.S., Bertsch, P.M., 2001. Immobilization of nickel and other metals in contaminated sediments by hydroxyapatite addition. J. Environ. Qual. 30 (2), 460–469.

Sheha, R.R., 2007. Sorption behavior of Zn(II) ions on synthesized hydroxyapatites. J. Colloid Interface Sci. 310 (1), 18–26.

Silvano, M., Alessia, C., Vincenzo, F., 2012. Evaluation of the effectiveness of phosphate treatment for the remediation of mine waste soils contaminated with Cd, Cu, Pb, and Zn. Chemosphere 86 (4), 354–360.

Smičiklas, I.D., Milonjić, S.K., Pfendt, P., Raičević, S., 2000. The point of zero charge and sorption of cadmium(II) ions on synthetic hydroxyapatite. Sep. Purif. Technol. 18 (3), 185–194.

Srinivasan, M., Ferraris, C., White, T., 2006. Cadmium and lead ion capture with three dimensionally ordered macroporous hydroxyapatite. Environ. Sci. Technol. 40 (22), 7054–7059.

Vila, M., Sánchez-Salcedo, S., Cicuéndez, M., Izquierdo-Barba, I., Vallet-Regí, M., 2011. Novel biopolymer-coated hydroxyapatite foams for removing heavy-metals from polluted water. J. Hazard. Mater. 192 (1), 71–77.

Xu, Y., Schwartz, F.W., Traina, S.J., 1994. Sorption of Zn^{2+} and Cd^{2+} on hydroxyapatite surfaces. Environ. Sci. Technol. 28 (8), 1472–1480.

Ye, X.X., Li, H.Y., Ma, Y.B., Wu, L., Sun, B., 2014. The bioaccumulation of Cd in rice grains in paddy soils as affected and predicted by soil properties. J. Soils Sediments 14 (8), 1407–1416.

Ye, X.X., Kang, S.H., Wang, H.M., Li, H.Y., Zhang, Y.X., Wang, G.Z., Zhao, H.J., 2015. Modified natural diatomite and its enhanced immobilization of lead, copper and cadmium in simulated contaminated soils. J. Hazard. Mater. 289, 210–218.

Zhang, Z.Z., Li, M.Y., Chen, W., Zhu, S.Z., Liu, N.N., Zhu, L.Y., 2010. Immobilization of lead and cadmium from aqueous solution and contaminated sediment using nano-hydroxyapatite. Environ. Pollut. 158 (2), 514–519.

Zheng, W., Li, X.M., Yang, Q., Zeng, G.M., Shen, X.X., Zhang, Y., Liu, J.J., 2007. Adsorption of Cd(II) and Cu(II) from aqueous solution by carbonate hydroxylapatite derived from eggshell waste. J. Hazard. Mater. 147 (1–2), 534–539.